RESEARCH ON THE PERFORMANCE OF HEAT STORAGE DEVICES UNDER DIFFERENT MELTING POINT PHASE CHANGE MATERIALS IN INDUSTRIAL WASTE HEAT UTILIZATION

by

Xingquan SONG*

College of Energy and Power Engineering, Dalian University of Technology,
Ganjingzi District, Dalian, Liaoning, China

Original scientific paper
https://doi.org/10.2298/TSCI250912180S

Phase change heat storage technology can provide effective solutions for temporal and spatial mismatch in the utilization of industrial waste heat and achieve efficient heat transportation. However, in view of the diverse characteristics of industrial waste heat, it is urgent to conduct research on the utilization of waste heat at different temperatures. Building upon existing theories, this paper innovatively establishes a numerical model for multi-melting-point phase change heat storage materials (PCMs), taking into account both temperature of the heating surface and melting points of the heat storage materials. The melting process of the selected materials was simulated and the results were discussed. The coupled thermal performance of different heating surfaces and melting point temperatures was quantitatively clarified based on the analysis of the results of numerical models. The research results show that different heating surfaces have remarkable influence on the melting efficiency. At the melting point of 50 ℃, under the heating surface at 75 ℃, the complete melting time is only 3360 seconds, which is 31% of the complete melting time when using a heating surface at 60 ℃. Furthermore, when the heating surface temperature reaches a certain level, the influence brought by melting point gradually diminishes. Evolution diagrams of the temperature field visually demonstrates the positive correlation between the intensity of natural convection and the heat transfer temperature difference. Finally, it was found that latent heat mainly determines the heat storage capacity of PCM and choose materials with appropriate melting points can improve the heat storage rate. By conducting research on the new type of heat storage device with multiple heating surfaces and multiple melting points, this study provides guidance for optimizing the heat utilization efficiency in practical engineering applications.

Key words: *PCMs, industrial waste heat utilization, melting performance, melting point*

Introduction

Given the non-renewability and environmental hazards of fossil energy, industrial waste heat [1] and other residual heat resources have received increasing attention [2]. How-

* Author's e-mail: songxqemail2024@163.com

ever, industrial waste heat has the characteristics of intermittency and difficult transportation [3]. Therefore, thermal energy storage technology is usually applied in practical engineering to achieve the effective utilization of waste heat.

At present, the commonly used heat storage methods include sensible heat storage [4], latent heat storage [5], and chemical energy storage [6]. Taking both safety and economy into consideration, latent heat storage is frequently applied in the reuse of industrial waste heat. Gioanola *et al*. [7] utilized a new pillow-type phase change thermal storage system through a dual-model collaborative design, providing a highly precise and cost-effective solution for large-scale industrial thermal storage. Nyallang Nyamsi *et al*. [8] designed a metal hydride dual-tank thermochemical energy storage device with PCM jacket. Their research verifies that the coordinated optimization of the PCM's thermal conductivity and melting point is the key to achieving efficient waste heat recovery. Yang *et al*. [9] designed a stepped latent heat device which provides key technical support for decarbonization of building heating.

Although PCMs are widely used in industrial waste heat (IWH) recovery and reuse, there are still issues such as heat balance [10] and heating matching [11]. In response to this, some scholars have conducted research on the melting properties of different PCMs (melting points and materials). Hu *et al*. [12] evaluated the application of a composite heat storage system composed of sodium acetate trihydrate and water in waste heat heating. The water-PCM system demonstrates good potential for off-peak electricity/solar energy heating applications. Yan and Mu [13] innovatively developed a binary PCM. It has the characteristics of a small supercooling degree and stable thermal performance, and can efficiently recover low-temperature industrial waste heat. Marri *et al.* [14] conducted experiments and numerical studies to investigate the influence of phase transition temperature on the melting efficiency of PCM-based heat sinks. They used three types of PCM with phase transition temperatures and found that the performance of PCM heat sinks with a higher phase transition temperature could be up to 2.25 times higher.

Furthermore, different heating temperatures also have corresponding effects on the heat storage performance of the PCMs [15]. Yang *et al*. [16] conducted experiments on wax-copper foam composite materials and found that an increase in the temperature of the heat transfer fluid (HTF) significantly enhanced the heat storage performance of the PCM by increasing the heat transfer temperature difference and strengthening the conduction/convection mechanism. However, it should be noted that the benefits diminish at high temperatures. Zheng and Wang [17] used numerical calculation model of PCM natural convection to reach the conclusion that when the temperature of the heat carrier fluid exceeds a certain range, the effectiveness of increasing the heat source temperature will weaken. Mosaffa *et al*. [18] analyzed the influence of the base temperature/heat flux of the fin under three boundary conditions on the solidification rate and temperature field. A decrease in the base temperature of the fin (*e.g*., from 14 °C to 7 °C) can increase the solidification rate by more than 40%, providing critical parameter thresholds for industrial design.

Based on the existing research results, it has been clearly pointed out that for different types of industrial waste heat recovery, further in-depth studies on the adaptability of PCMs with different melting points are needed. At the same time, the melting performance of PCMs under various thermal conditions still lacks comprehensive and systematic exploration. Therefore, in this study, an innovative numerical model of multi-melting-point phase change heat storage materials was constructed. Focusing on key parameters such as complete melting time, temperature field distribution, phase interface evolution, and heat storage capacity, the performance of heat storage devices in industrial waste heat utilization was systematically

studied, providing more targeted reference value for the precise matching of different melting-point heat storage materials in practical engineering applications.

Methodology

Problem description and physical model

The phase change heat storage (PCHS) devices can be used in the recovery and utilization of IWH. As shown in fig. 1, the process of industrial waste heat being transported from the factory to residents through a box-shaped heat storage device mainly consists of three parts: IWH recovery, PCHS device, and IWH utilization. The high temperature IWH, after passing through the heat exchanger, generates a heat fluid of suitable temperature, which

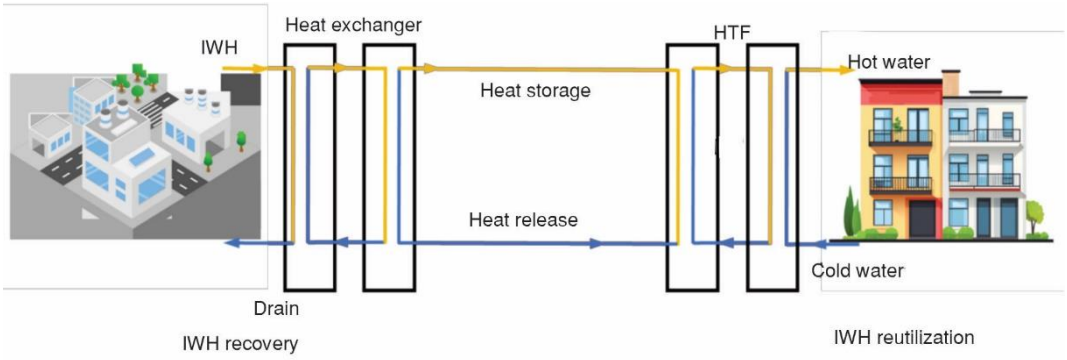

Figure 1. Schematic diagram of the principle of heat storage and recovery, transportation, and reuse in auxiliary heating of the building

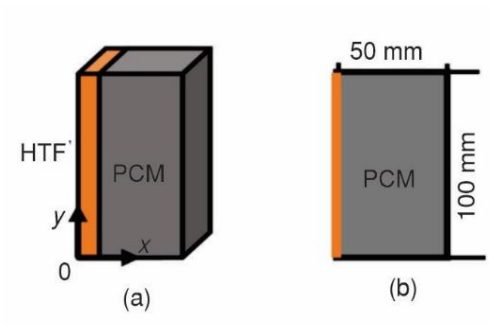

Figure 2. Physical model of phase change heat storage; (a) schematic diagram of the PCHS device and (b) 2-D numerical model (length: 100 and width: 50)

is used in the PCHS process. After being stored in the PCHS device, it is transported to the end users of residents for releasing heat, which is used for heating and the preparation of domestic hot water. Throughout the entire process of IWH utilization, the PCHS device plays a significant role and determines the efficiency of heat for utilization. Therefore, this study focused on the melting performance of the PCHS device. Since the PCHS devices are used in parallel, a single phase change reservoir was selected for characterization, and the heat storage model is shown in fig. 2. In fig. 2(a), the thermal fluid of the PCHS device flows on the left side, while the PCM is on the right side. According to the model properties, it is simplified to a 2-D model as shown in fig. 2(b), with a model size of 20 mm × 50 mm. Wax is selected as the PCM, and its properties are as shown in tab. 1. To study the utilization of IWH under different temperatures, we used different melting points of PCM for matching and investigated the melting performance of the device. The research case is shown in tab. 2.

Mathematic model

To solve the numerical model, this study used COMSOL 6.2.0.290 to build the model and conduct the solution. The main assumptions are [19]:

- The material properties do not change with temperature, and it is assumed that the material is uniformly filled. The settings are as shown in tab. 1.
- During the phase transformation process, the volume changes of the material are ignored.
- Ignoring the undercooling of the material, the melted material is assumed to follow the Boussinesq hypothesis.

Table 1. The thermal physical properties of PCM (including both solid and liquid phases)

Material properties	Melting temperature	Specific heat capacity	Latent heat	Thermal conductivity	Density	Coefficient of thermal expansion	Viscosity
Unit	K	J/kgK	J/kg	W/mK	kg/m³	1/K	Pa·s
Value	323.15-327.15	2400(s)/ 3200(l)	2.40×10^{05}	0.2(s)/0.1(l)	800(s)/ 800(l)	0.0058333	0.00689

Table 2. Numerical model case; case-heating wall [°C] and melting point [°C]

Case	Heating wall, Melting point	Case	Heating wall, Melting point	Case	Heating wall, Melting point	Case	Heating wall, Melting point
Case A-1	60, 30	Case B-1	65, 30	Case C-1	70, 30	Case D-1	75, 30
Case A-2	60, 35	Case B-2	65, 35	Case C-2	70, 35	Case D-2	75, 35
Case A-3	60, 40	Case B-3	65, 40	Case C-3	70, 40	Case D-3	75, 40
Case A-4	60, 45	Case B-4	65, 45	Case C-4	70, 45	Case D-4	75, 45
Case A-5	60, 50	Case B-5	65, 50	Case C-5	70, 50	Case D-5	75, 50
Case A-5	60, 50	Case B-5	65, 50	Case C-5	70, 50	Case D-5	75, 50

Melting is a process that changes over time thus transient numerical simulation is required. After constructing the model, the solution is obtained by solving the control equations eqs. (1)-(11):

$$\rho c_p \boldsymbol{u} \nabla T + \nabla \left(\dot{\boldsymbol{q}}_c + \dot{\boldsymbol{q}}_r \right) = \beta T \left(\frac{\partial p}{\partial t} + \boldsymbol{u} \nabla p \right) + \tau : \nabla \boldsymbol{u} + Q \tag{1}$$

The numerical model used to solve the flow field [20] in eqs. (2) and (3). An additional item needs to be introduced, $S(T)\boldsymbol{u}$, to simulate the transitional zone between the solid phase and the liquid phase:

$$\rho \nabla \boldsymbol{u} = 0 \tag{2}$$

$$\rho\frac{\partial \boldsymbol{u}}{\partial t}+\rho(\boldsymbol{u}\nabla)\boldsymbol{u}=\nabla\left[-p\boldsymbol{I}+\mu\left(\nabla\boldsymbol{u}+(\nabla\boldsymbol{u})^{T}\right)\right]+\boldsymbol{F_B}-S(T)\boldsymbol{u} \tag{3}$$

The buoyancy force, $\boldsymbol{F_B}$, causes natural convection. Its value is calculated using the Boussinesq eq. (4). The rationality of the application of this equation has been explained in the model assumptions:

$$\boldsymbol{F_B}=-\rho_l\beta\mathrm{g}\left(T-T_{pc}\right) \tag{4}$$

The phase transition is characterized by the melting fraction, φ, according to eq. (5). The parameter phase transition temperature range, ΔT_{pc}, defines the extent of the transition region:

$$\begin{gathered}\varphi(T)=0 \ \text{ for } \ T<T_{pc}-\frac{\Delta T_{pc}}{2}\\ \varphi(T)=\frac{T-\left(T_{pc}-\dfrac{\Delta T_{pc}}{2}\right)}{\Delta T_{pc}} \ \text{ for } \ T_{pc}-\frac{\Delta T_{pc}}{2}<T<T_{pc}+\frac{\Delta T_{pc}}{2}\\ \varphi(T)=1 \ \text{ for } \ T<T_{pc}+\frac{\Delta T_{pc}}{2}\end{gathered} \tag{5}$$

Equation (6) defines the additional source term, $S(T)$, which includes the Kaman-Chozeni relationship, referring to the flow resistance term in the turbid zone. Among the numerical modeling, the key coefficient of the fuzzy zone, A_m, plays a decisive role in the calculation results. The constant, ε = 0.001, can prevent the occurrence of division-by-zero errors when is present:

$$S(T)=A_m\frac{\left(1-\varphi(T)\right)^2}{\varphi(T)^3+\varepsilon} \tag{6}$$

The melting fractions of the solid region and the transition region, $\varphi(T) < 1$, which will result in a larger source term, $S(T)$, depend specifically on the value of the amorphous zone coefficient, A_m. Therefore, the fluid-flow in the solid region is completely blocked, while the flow in the transitional region between the solid and liquid phases will be weakened.

The phase change physical model is implemented according to [21] using custom functions and material properties. Through the custom functions, the physical parameters of solid and liquid PCM as well as the flow characteristics in the transition zone are described. The melting fraction, $\varphi(T)$, is used to characterize the temperature-dependent material properties: The density, $\rho(T)$, is obtained according to eq. (7), and the thermal conductivity, $\lambda(T)$, is determined similarly based on eq. (8):

$$\rho(T)=\rho_s+\left(\rho_l-\rho_s\right)\varphi(T) \tag{7}$$

$$\lambda(T)=\lambda_s+\left(\lambda_l-\lambda_s\right)\varphi(T) \tag{8}$$

To define the viscosity, $\mu(T)$, related to the phase, in addition to using the source term, $S(T)$, an auxiliary constant, ξ = 1 m^2, was introduced, as shown in:

$$\mu(T) = \mu_l + S(T)\xi \tag{9}$$

The heat capacity method defines the phase transition by using the corrected specific heat capacity. The latent heat is a characteristic quantity of the phase transition. Here, the Gaussian function of eq. (10) is adopted, which is centered around the phase transition temperature, T_{pc}:

$$D(T) = \frac{\mathrm{e}^{-\frac{\left(T-T_{pc}\right)^2}{\left(\frac{\Delta T_{pc}}{4}\right)^2}}}{\sqrt{\pi\left(\frac{\Delta T_{pc}}{4}\right)^2}} \tag{10}$$

Calculate the corrected specific heat capacity, cp(T), based on eq. (11) to maintain energy balance during the process:

$$c_p(T) = c_{p,s} + \varphi(T)\left(c_{p,l} - c_{p,s}\right) + LD(T) \tag{11}$$

Initial conditions and boundary conditions

To ensure the uniformity of the model, we set the boundary conditions and initial conditions as:

- The initial temperature of the PCM and the ambient temperature are both 25º.
- The heating boundaries were set at 60 °C, 65 °C, 70 °C, and 75 °C according to the simulation cases, while the other boundaries were regarded as adiabatic.

Verification

To ensure the accuracy of the calculation results and the efficiency of resource utilization, we conducted the grid independence verification for the spatial distribution of the melting rate in Case A-2, using 10532, 22783, and 45952 computational units for comparative analysis. The research results show that when the number of grids is increased to 22789 units, the deviation of the calculation results from the high-precision benchmark model (45952 units) is controlled within 2%, fig. 3(a). In contrast, the coarse grid model (10532 units) shows significant errors, with a difference exceeding 8%, confirming that its resolution is insufficient to

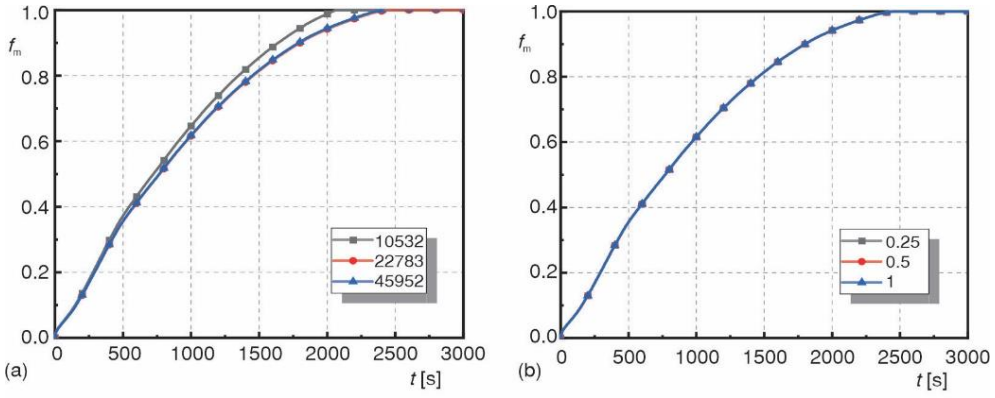

Figure 3. Independence verification; (a) grid numbers and (b) time step

support reliable predictions. Therefore, 22783 units were determined to be the optimal grid configuration that meets the accuracy requirements. In the verification of time step independence, we tested three time step settings: 0.25 seconds, 0.5 seconds, and 1.0 seconds. The experimental data showed that when using a 0.5 seconds time step, the accuracy was higher, and it also effectively reduced the consumption of computing resources. Based on the above dual verification results, the final combination scheme of 10532 computing units and 0.5 seconds time step was established.

Results and discussion

Complete melting time

Figure 4 shows the complete melting time of the phase change heat storage material under heating conditions of 60 ℃, 65 ℃, 70 ℃, and 75 ℃. It compares the PCHS efficiency at melting point temperatures of 30 ℃, 35 ℃, 40 ℃, 45 ℃, and 50 ℃. In fig. 4(a),

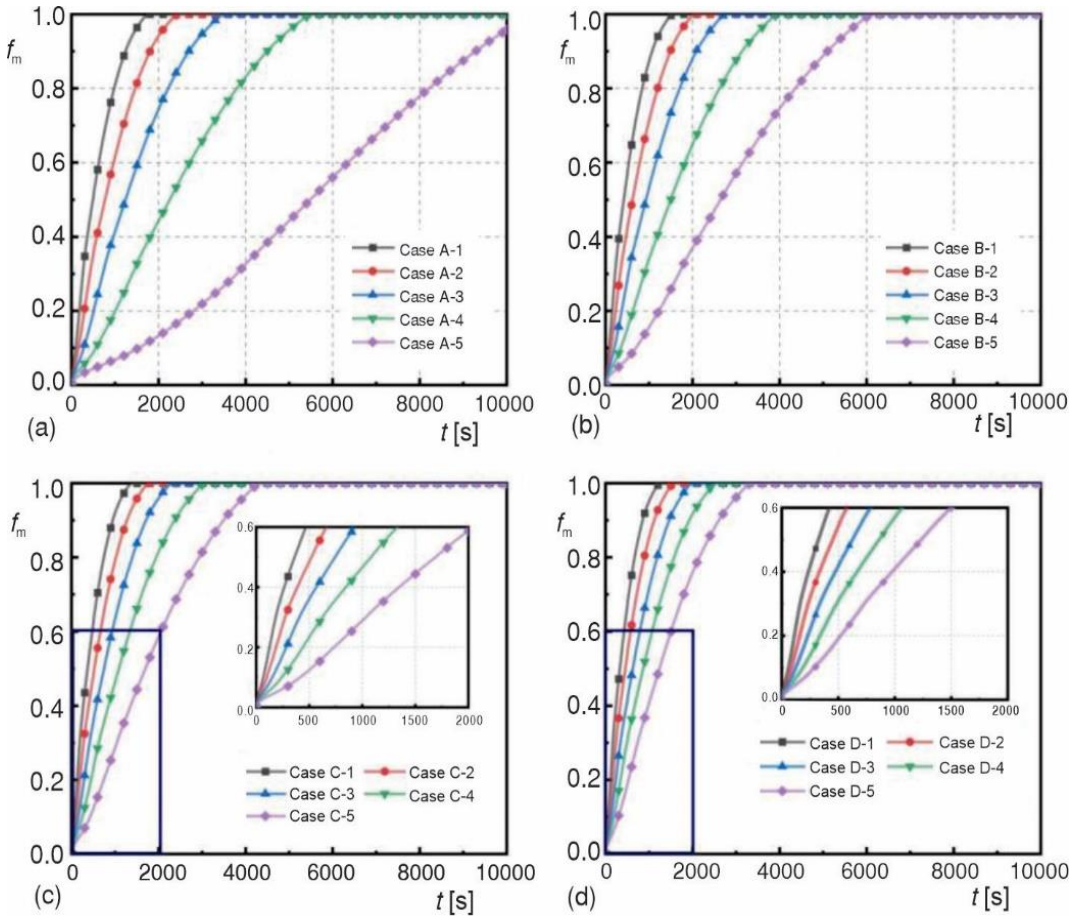

Figure 4. Comparison of the complete melting time of multi-melting-point phase change heat storage materials under different heating surfaces; (a) 60 ℃, (b) 65 ℃, (c) 70 ℃, and (d) 75 ℃

the complete melting time of Case A-1 is the shortest, at only 1790 seconds. It is followed by Cases A-2, A-3, and A-4, with Case A-5 being the last. Based on the case of a melting point of 50 ℃ (t_{full} = 10810 seconds), the complete melting times of the PCMs at 30 ℃, 35 ℃, 40 ℃, and 45 ℃ were shortened by 83%, 77%, 67%, and 48%, respectively. Meanwhile, during the initial stage of the phase change heat storage process, the PCM is in a solid state and mainly relies on conduction for heat transfer.

A large temperature difference is conducive to the continuous progress of the melting process, and the difference in melting rates among phase change heat storage materials with different melting points gradually emerges. In the later stage of melting, due to the increase in the amount of PCM in the liquid phase, the heat transfer process not only relies on conduction but also is strongly influenced by natural convection.

In fig. 4(b), with Case B-5 as the reference (the complete melting time is 6170 seconds), the melting efficiencies of Cases B-1, B-2, B-3, and B-4 have increased by 75%, 66%, 55%, and 35%, respectively. Similarly, for Cases C-1, C-2, C-3, and C-4, the charging time was reduced by 68%, 59%, 47%, and 29%, respectively, compared to Case C-5. Among them, the charging time of Case C-5 was 4360 seconds. In Case D, Case D-1 was the fastest, taking 1270 seconds. This was a 62% reduction compared to Case D-5. Furthermore, the difference in heat storage efficiency between the phase change heat storage device with a melting point of 50 ℃ (the highest) and the one with a melting point of 45 ℃ (the second highest) is gradually narrowing, and this is particularly evident in Group D. Therefore, at lower heating temperatures, low-melting-point heat storage materials can be selected to improve the heat storage efficiency. In the high temperature heating area, the influence of the melting point temperature within the research range gradually decreases. In this case, it is advisable to choose appropriate phase change heat storage materials for industrial waste heat recovery, providing theoretical value for practical engineering applications.

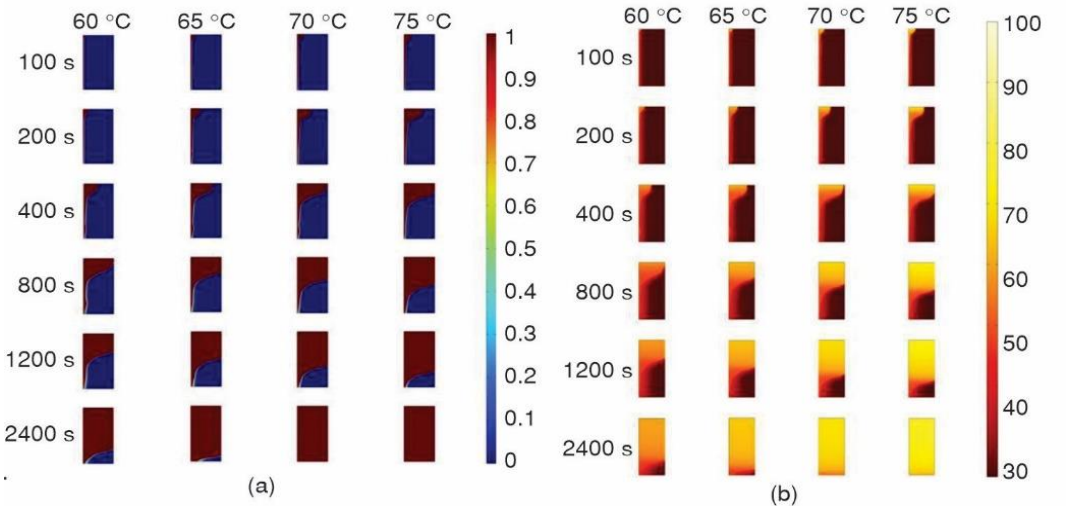

Figure 5. The 40 ℃ melting-point PCMs under various heating surfaces; (a) phase interface evolution and (b)temperature field
(*for colour image see journal web site*)

Interface and temperature field distribution

Figure 5(a) shows the phase interface evolution process of the 40 °C melting-point phase change heat storage device at different heating surface temperatures (60 °C, 65 °C, 70 °C, 75 °C) at times t = 100 seconds, 200 seconds, 400 seconds, 800 seconds, 1200 seconds, and 2400 seconds (red: liquid paraffin; blue: solid paraffin). Overall, the interface forms a funnel shape and continuously expands over time, eventually melting completely. At t = 100 seconds, this is the initial stage of melting. Conduction dominates the heat transfer process, and only the wax around the heating surface melted. The shapes of the phase interfaces under the four heating surfaces do not differ much. From 200-800 seconds, the paraffin in the device gradually melted, and the increase in the liquid PCM enhanced the natural convection effect of the device, making the difference more obvious. Based on the funnel shapes of the phase interfaces at different temperature differences, and the natural convection effect is the strongest at 75 ℃. At the end of the charging stage, a refractory area appeared at the bottom of the PCHS device, far from the heating surface. At 2400 seconds, the heat storage units with a heating surface temperature of 70 ℃ and 75 ℃ had completely melted, the heat storage unit with a temperature of 65 ℃ was basically melted, while the refractory area at the bottom was larger and also the cause of the long heat storage.

To further visually analyze the impact of temperature difference on the melting performance, fig. 5(b) presents the distribution of temperature for the 40 ℃ melting-point PCM under different heating surfaces. Similarly, it can be observed that as the temperature of the heating surface increases, the temperature of the entire heat storage device also rises. In the temperature distribution, the temperature gradient is similar to the distribution of phase interfaces. There is a significant temperature difference between the solid and the liquid. Therefore, there is natural convective heat transfer between molten paraffin and solid paraffin. From 200-400 seconds, in the molten wax, the high heat transfer temperature difference also led to poor temperature uniformity. The top temperature of the high temperature heating surface was higher, which was the reason for the rapid melting at the top of the heat storage device. At the end of the melting process, due to the large amount of heat generated by the high-temperature heating surface, the device completed melting first and entered the exothermic heat storage stage, quickly achieving uniform temperature.

Figure 6(a) shows the distribution of the phase interface of the PCHS device at 65 ℃ under different melting points (30 ℃, 35 ℃, 40 ℃, 45 ℃, 50 ℃). Consistent with the time scale in fig. 5 and similarly, in the initial stage of melting, heat conduction dominates. Later, the increase in the amount of molten PCMs triggers natural convection, causing the interface to develop asymmetrically into a funnel shape. This shape expands continuously over time and eventually reaches the maximum melting degree. Based on the shape of the phase interface funnel corresponding to different melting points, it can be observed that the PCM with a melting point of 30 ℃ exhibits the strongest natural convection effect. This is attributed to its lower melting point, which results in a greater temperature gradient in the molten zone at the same heating temperature (65 ℃), thereby enhancing the natural convection effect. At the end of the melting process, the phase change heat storage device exhibits a region of difficult-to-melt material at the bottom of the storage device, away from the heating surface. By analyzing this phenomenon, it can be known that for high-melting-point materials, the thermodynamic driving force (lift force) for driving natural convection at a given heating temperature is relatively weak, which leads to a decrease in the heat transfer efficiency in the bottom area.

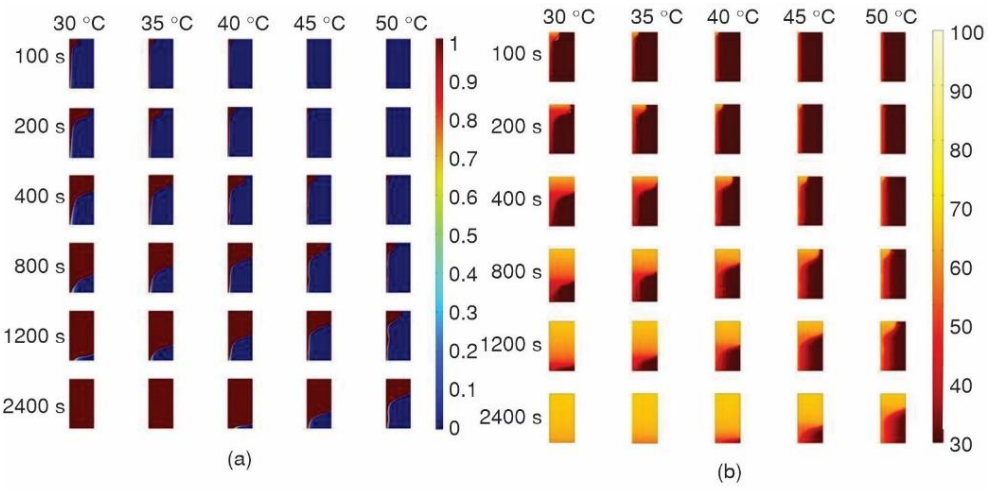

Figure 6. The 65 °C heating surface phase change heat storage device at different melting points; (a) phase interface evolution and (b)temperature field (*for colour image see journal web site*)

Consequently, the temperature distribution characteristics within the PCM clearly confirm the aforementioned differences in the intensity of natural convection. Figure 6 shows the temperature distribution of different PCMs with different melting points under a 65 °C heating surface, which is consistent with the selected time slice in fig. 6(b). The temperature of the PCHS device rises as the temperature increases. For the temperature distribution, the temperature gradient is similar to the distribution of phase interfaces. There is a significant temperature difference between the solid and the liquid. The materials with melting points of 30 °C and 35 °C achieved the fastest temperature uniformity. However, at 45 °Cand 50 °C, significant temperature boundaries emerged later due to the presence of large areas with difficult-to-melt regions. For PCM with lower melting points, a larger temperature difference in the heat transfer surface leads to a stronger natural convective heat transfer effect. At the same heating surface temperature, the PCHS units with lower melting points will have a higher melting efficiency. For materials with higher melting points, the overall temperature distribution is relatively uniform and the temperature gradient is gentle. The temperature contour lines are relatively sparse, indicating that the thermal boundary layer is thick, the natural convection is weak, and the heat transfer relies more on the less efficient heat conduction mechanism.

Comparison of PCHS capacity

Based on the previous research results, to further discuss the impact of different melting points on the PCHS capacity, we compared the complete melting time, heat storage capacity and PCHS speed of the PCHS process at different melting points under a 65 °C heating surface, as shown in fig. 7. During the complete melting period, the results are consistent with those presented in fig. 4. Among them, the complete melting time of Case B-1 is the shortest, while the longest is that of Case B-5. In terms of heat storage capacity, due to the similarity in shape and material properties of the phase change heat storage devices. Furthermore, the sensible heat only accounts for one quarter of the total PCHS capacity, indicating that the capacity of the PCM mainly lies in latent heat. Therefore, increasing the temperature

of the heating surface has a relatively little influence on enhancing the heat storage capacity. Hence, it is more important to focus on the heat storage rate. In terms of the PCHS rate, it was found that the PCHS rate of Case B-1 was the highest, which was 2.9 times higher than that of Case B-5.

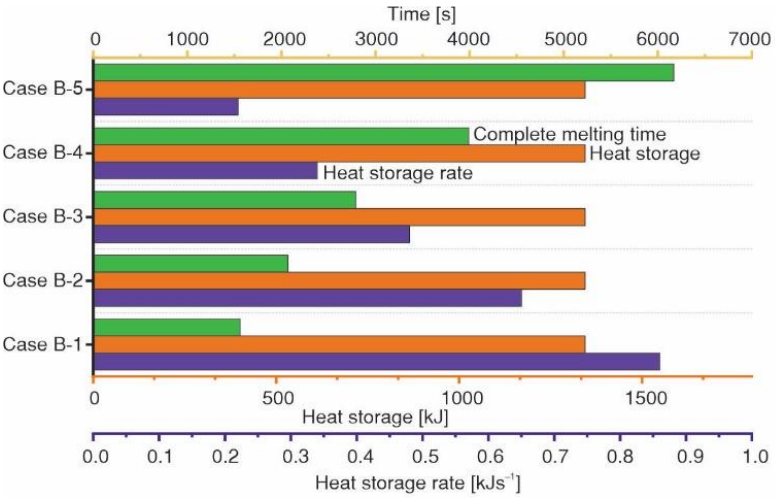

Figure 7. Comparison of heat storage capacity of the heating surface under different melting points

Conclusions

In this research, we innovatively employed multiple sets of phase transition material melting points and heating surface temperatures to investigate melting characteristics under different heating conditions. Here are the main conclusions as follows.

- The melting rate of PCM is significantly influenced by both its melting point and the temperature of the heating surface. A lower melting point can significantly shorten the charging time, and the lower the temperature, the more pronounced this effect becomes. Among them, the difference in the charging efficiency of the PCMs with different melting points under the 60 °C heating surface was the most significant.
- At the same melting point, the heat storage rate of the high heating surface is higher, and the time difference for complete melting at different melting points under the high heating surface is shortened. Under these conditions, heat storage materials suitable for the user's melting point can be selected.
- The evolution law of the temperature field indicates that the intensity of natural convection is dominated by the temperature difference of heat transfer, which in turn affects the morphology of the interface and the melting efficiency.
- The heat storage capacity of phase change heat storage materials is mainly dominated by latent heat. The increase in heating surface temperature has a limited effect on the total heat storage capacity. Under a constant heating surface, a lower melting point material can be appropriately selected to pursue an increase in the heat storage rate.

This article presents the heat storage performance of multiple heating surfaces at different melting points, which can be applied in practical engineering guidance. However, this paper only studied the melting phase transition process and did not set up a solidification

group to form a control group, thus unable to comprehensively reflect the actual operating performance of the cycle. Meanwhile, the application of the research results in actual industrial systems still requires further verification through experiments. In the subsequent research, we will add research on the solidification process and evaluate the cyclic working performance of the phase change system. Furthermore, we will set more complex and comprehensive material properties and boundary conditions to provide parameter threshold references for industrial applications.

References

[1] Kosmadakis, G., Industrial Waste Heat Potential and Heat Exploitation Solutions, *Applied Thermal Engineering, 246* (2024), 122957
[2] Montella, L., *et al*., An Integrated Multi-Criteria Decision Making Framework for Industrial Excess Heat Recovery and Utilization, *Energy, 318* (2025), 134721
[3] Nomura, T., *et al*., Waste Heat Transportation System, Using Phase Change Material (PCM) from SteelWorks to Chemical Plant, *Resources, Conservation and Recycling, 54* (2010), 11, pp. 1000-1006
[4] Anacreonte, A. V., *et al*., Impact of Inlet Fluctuations on the Stratification of a Sensible Thermal Energy Storage, *Renewable Energy, 252* (2025), 123484
[5] Ghosh, D., *et al*., Strategies for Phase Change Material Application in Latent Heat Thermal Energy Storage Enhancement: Status and Prospect, *Journal of Energy Storage, 53* (2022), 105179
[6] Yang, X., *et al*., Numerical Study of $Mg(OH)_2/MgO$ Thermochemical Heat Storage Reactor Coupled with Parabolic Dish Solar System, *Applied Thermal Engineering, 261* (2025), 125128
[7] Gioanola, G., *et al*., Innovative Methodology for Optimized Design and Thermo-Economic Analysis of Pillow-Plate Latent Heat Thermal Energy Storage: A Case Study on Heat Recovery in the Brewing Industry, *Energy Conversion and Management, 341* (2025), 120025
[8] Nyallang Nyamsi, S., *et al*., Metal Hydride Beds-Phase Change Materials: Dual Mode Thermal Energy Storage for Medium-High Temperature Industrial Waste Heat Recovery, *Energies, 12*, (2019), 20, 3949
[9] Yang, S., *et al*., A Novel Cascade Latent Heat Thermal Energy Storage System Consisting of Erythritol and Paraffin Wax for Deep Recovery of Medium-Temperature Industrial Waste Heat, *Energy, 265* (2023) 126359
[10] Marambio, M. A., *et al*., Surface Melting of Snow-Firn-Ice Structures and Estimation of Extended Transient Energy and Mass Balances Using a Liquid Solid Phase-Change Model, *International Communications in Heat and Mass Transfer, 136* (2022), 106175
[11] Yang, X., *et al*., Enhanced Coupling of Low-Grade Heat Sources with Carnot Battery Through Optimal Temperature Matching, *Energy Conversion and Management, 339* (2025), 119953
[12] Hu, B., *et al*., Experimental and Numerical Investigation on Heating Performance Comparison of Air Conditioning Heating Systems Based on Water-Phase Change Material Heat Storage System and Water Heat Storage System, *Energy, 331* (2025), 137005
[13] Yan, Q., Mu, B., Energy Storage Materials for Phase Change Heat Devices Recovering Industrial Waste Heat for Heating Purposes, *International Communications in Heat and Mass Transfer, 160* (2025), 108376
[14] Marri, G. K., *et al*., Effect of Phase Change and Ambient Temperatures on the Thermal Performance of a Solid-Liquid Phase Change Material Based Heat Sinks, *Journal of Energy Storage, 30* (2020), 101327
[15] Yu, M., *et al*., Numerical Simulation Study of Heat Transfer Fluid Boiling Effects on Phase Change Material in Latent Heat Thermal Energy Storage Units, *Energies, 18* (2025), 14, 3836
[16] Yang, J., *et al*., Experimental Study on Enhancement of Thermal Energy Storage with Phase-Change Material, *Applied Energy, 169* (2016), May, pp. 164-176
[17] Zheng, Y., Wang, Z., Study on the Heat Transfer Characteristics of a Shell-and-Tube Phase Change Energy Storage Heat Exchanger, *Energy Procedia, 158* (2019), Feb., pp. 4402-4409
[18] Mosaffa, A., *et al*., Green's Function Solution for Transient Heat Conduction in Annular Fin During Solidification of Phase Change Material, *Applied Mathematics and Mechanics, 33* (2012), 10, pp. 1265-1274

[19] Sabine, M., Robert, D., Influence of Natural Convection and Volume Change on Numerical Simulation of Phase Change Materials for Latent Heat Storage, *Energies, 15* (2022), 8, 2746
[20] Oertel, H., Bohle, M., *Prandtl-Führer durch die Strömungslehre*, Springer, Amsterdam, The Netherlands, Vol. 10, 2001
[21] Kheirabadi, A. C., Groulx, D., Simulating Phase Change Heat Transfer Using COMSOL and FLUENT: Effect of the Mushy-Zone Constant, *Com. Thermal Sciences, 7* (2015), 5-6, pp. 427-440

Paper submitted: September 12, 2025
Paper revised: September 29, 2025
Paper accepted: October 1, 2025